

AFRL-SR-BL-TR-98-

es, gathering  
; collection of  
Highway, Suite

19981113 054

# Glass-Forming Liquid Crystals for Photonic Devices

## Table of Contents

1	INTRODUCTION.....	2
2	TECHNICAL OBJECTIVES .....	2
3	RESULTS AND DISCUSSION.....	3
3.1	MATERIALS SYNTHESIS .....	3
3.2	MATERIALS PROCESSING.....	6
3.3	OPTICAL PROPERTIES .....	7
3.4	DEVICE DEMONSTRATION .....	14
3.4.1	<i>Twisted Nematic (TN) Latching Switch</i> .....	14
3.4.2	<i>Latching Parallel-Aligned GLC Device</i> .....	15
3.5	TECHNOLOGY APPLICATION.....	16
3.6	MATERIALS DESIGN .....	16
4	CONCLUSIONS .....	17
5	REFERENCES.....	17

## 1 Introduction

This report summarizes the technical results on the Phase I STTR research program entitled Glass-Forming Liquid Crystals for Photonic Devices. On this program Cornerstone Research Group, Inc. (CRG) investigated the potential use of a new class of liquid crystal (LC) material developed at the University of Rochester (UR) for electrooptic applications. The material, referred to as a glass-forming liquid crystal (GLC), was developed by the Center for Optoelectronics & Imaging at the UR for use as large area passive optical components on the fusion laser program.

Glass-forming liquid crystals are a unique class of materials. At room temperature, they are solid and have the properties of a hard plastic. At temperatures above the glass transition temperature,  $T_g$ , they are fluid and behave as a conventional nematic LC until the temperature exceeds the clearing temperature,  $T_c$ , at which point a GLC becomes an isotropic fluid.

In this program, we postulated that it might be possible to align a thin film of GLC using an electric field at elevated temperatures and freeze in a desired molecular orientation by allowing the film to cool below  $T_g$ . This would allow an optical device based on the GLC materials technology to be investigated under this program to be electronically set to a desired optical state without need for continuous electrical power. Such a capability in electrooptic devices would be both unique and highly desirable for several electrooptic applications, such as routing fiber-optic signals.

## 2 Technical Objectives

The overall objective of the Phase I research effort was to demonstrate the feasibility of latching photonic devices based on GLC materials. This is a relatively new class of materials, which to our knowledge, had not been considered for active photonic device applications. In the Phase I effort, the University of Rochester synthesized GLC materials for evaluation. Cornerstone Research Group, Inc. characterized the electro-optical properties of these materials and demonstrated a latching photonic device. The stated objectives for the Phase I effort included:

1. Preparation of nematic GLC materials and thin films for characterization in terms of order parameter ( $S$ ), index of refraction ( $n$ ), optical birefringence ( $\Delta n$ ), dielectric anisotropy ( $\Delta\epsilon$ ), and response time to an applied field.
2. Experimental determination of the kinetics of defect formation and annihilation with an objective of accomplishing monodomain nematic glassy films via molecular design and film processing.
3. Identify the limits which GLCs can achieve in the context of the proposed technology, and investigate the design and synthesis route for improved GLC materials for Phase II.
4. Fabricate a series of GLC cells for performance assessment. At least three cell configurations shall be investigated. These include transmissive and reflective tunable birefringent cells, and a twisted nematic cell.
5. Characterize the optical performance of these devices in relation to the ultimate applications.
6. Investigate drive mechanisms for heating and switching the GLC cell simultaneously.
7. Assess the potential of GLCs for latching photonic devices.

To meet the needs of the device designs proposed in this program, nematic GLC materials with the following desired properties are needed:

- $T_g$  above 60°C with superior morphological stability
- A wide nematic temperature range with a  $T_c$  of at least 120 °C

- A high degree of molecular alignment and order with surface treatment
- High optical birefringence
- Low optical loss by absorption or scatter from 800 – 1600 nm
- Low  $dn/dT$  below  $T_g$ .

### 3 Results and Discussion

#### 3.1 Materials Synthesis

Prior research efforts at the University of Rochester has synthesized four materials to date, depicted as Compounds (I) through (IV) in Figure 1, that meet most of the above requirements. First, these materials were readily vitrifiable upon cooling, and a subsequent heating scan revealed a  $T_g$  between 60 and 80°C and a  $T_c$  between 120 and 200°C. Additional DSC and thermal annealing experiments indicated superior morphological stability against recrystallization. In addition, these nematic GLC's contain pendant groups with a relatively high optical birefringence,  $0.23 < \Delta n < 0.45$ . The observation that a 14-micrometer film of Compound (I) sandwiched between a pair of calcium fluoride substrates is transparent in a wide spectral region (from 400 to 2500 nm) is very encouraging as well (see Figure 2).

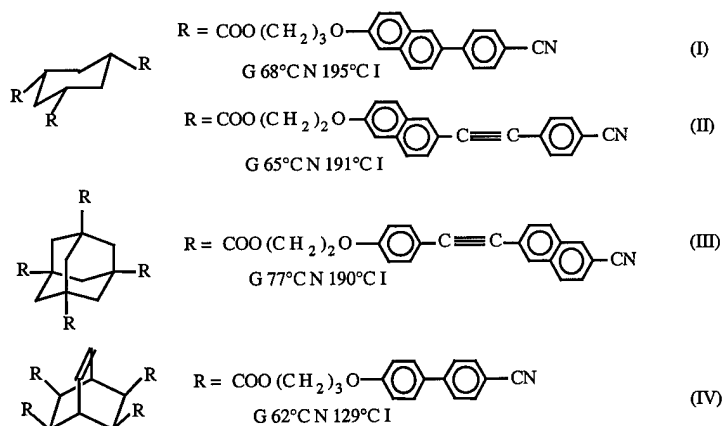


**Figure 1: Chemical structure of several nematic GLC materials synthesized.**

During a two-day kickoff meeting discussions were held to determine which materials would be experimentally assessed during this Phase I program. Based on these discussions GLC-IV and GLC-I were synthesized and evaluated. GLC-IV was synthesized first because the chemical precursors for this material are commercially available which significantly speeded up the synthesis process. The second material evaluated during the Phase I effort was GLC-I. This material was selected because it had significantly different chemical structure chemical properties, such as a higher  $T_g$  and wider nematic range. The University of Rochester synthesized and delivered approximately 2 grams each of GLC-IV and GLC-I to CRG for experimental studies. Figure 3 and 4 show the DSC data from each of these materials.

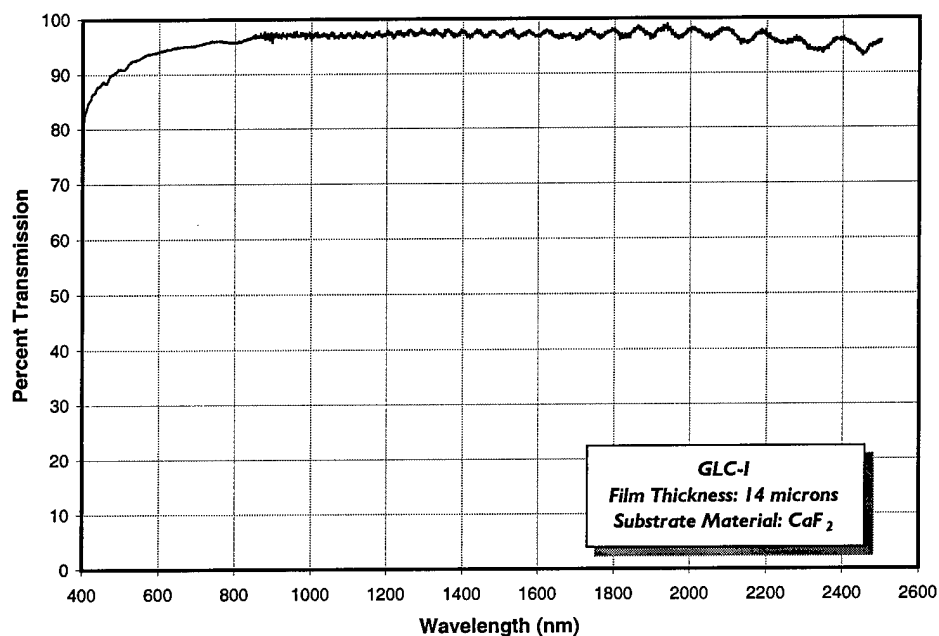


Figure 2: Vis-NIR transmission spectra of GLC-I between CaF<sub>2</sub> substrates.

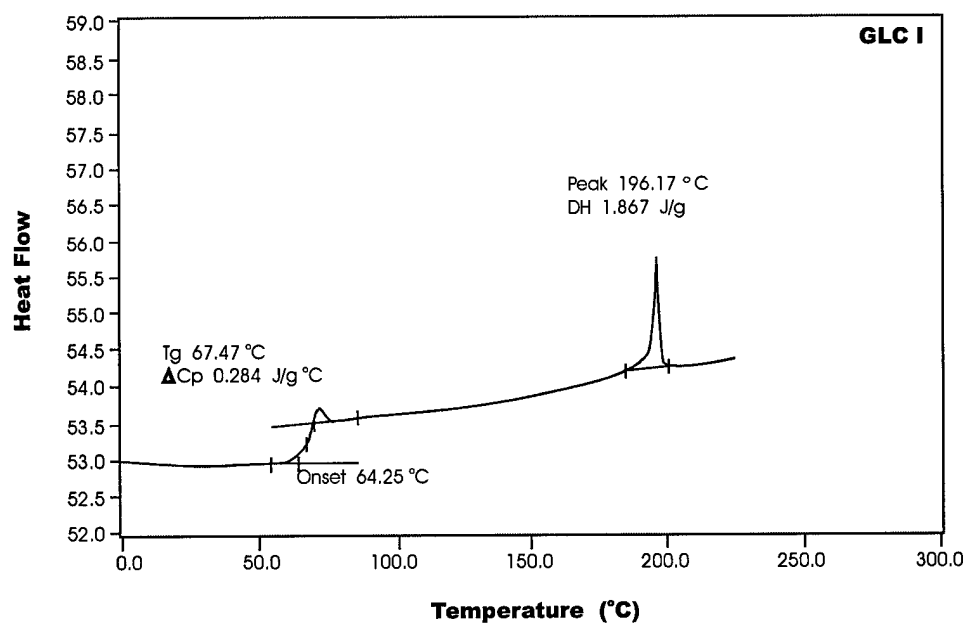
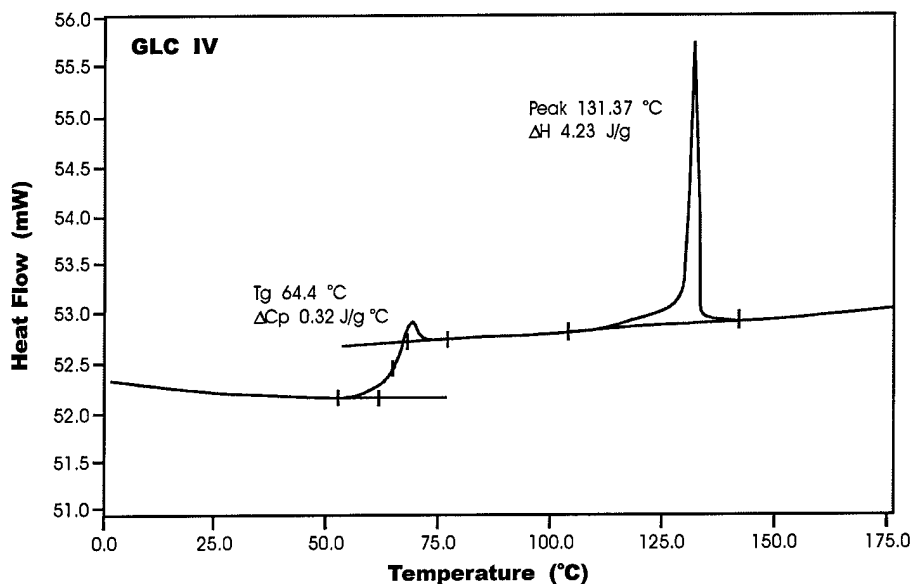
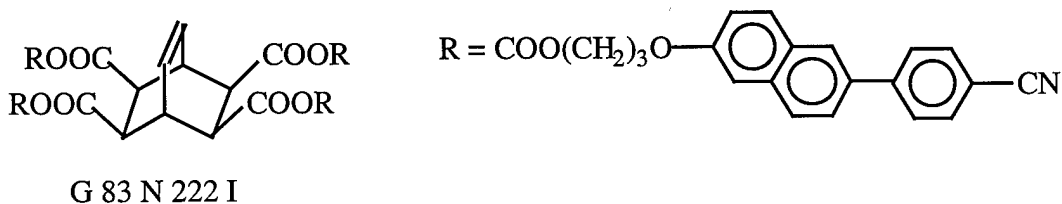


Figure 3: DSG measurement of pure GLC-I.



**Figure 4: DSC measurement of pure GLC-IV.**

In addition to these two materials, a new alternative nematic GLC compound with an adamantane core, as depicted in Figure 5, was synthesized, and DSC analysis showed a  $T_g$  at 83 °C and  $T_c$  at 222 °C. The high clearing temperature of this new class of GLC material may provide improved switching speed performance at the higher operating temperatures. Based on the research to date at UR, adamantane core is the best of all four that have been successfully integrated into GLC materials: cyclohexane, bicyclooctene, adamantane, and cubane. As the key intermediate, adamantanetetracarboxylic acid is commercially unavailable. To furnish potentially superior material candidates, in-house synthesis capability has been established. During the Phase I effort CRG was unable to assess this material's electrooptic properties due to time and funding limitations.



**Figure 5: Chemical structure of new nematic GLC material with adamantane core.**

Preliminary studies on the first GLC material delivered (GLC-IV) indicated that electrical switching was slow, even at temperatures approaching up to the clearing temperature, 125°C. In addition, the voltages needed to induce any optical effect were quite high (~50V). For these reasons a mixture study was undertaken to determine if the addition of a LMM-LC could reduce the switching temperature and voltage while still maintaining a latching capability below 50°C. These studies indicated that 70% GLC-I and 30% ZLI-1840 resulted in switching voltages below 10V with short-term latching below 50°C. Subsequent DSC analysis (see Figure 6) indicated the  $T_g$  of this material mixture to be below room temperature which allowed any GLC devices to relax over time at room temperature. Additional experiments used an 80/20 mixture which has a  $T_g$  slightly above room temperature. Figure 7 shows the DSC data for this 80/20 mixture.

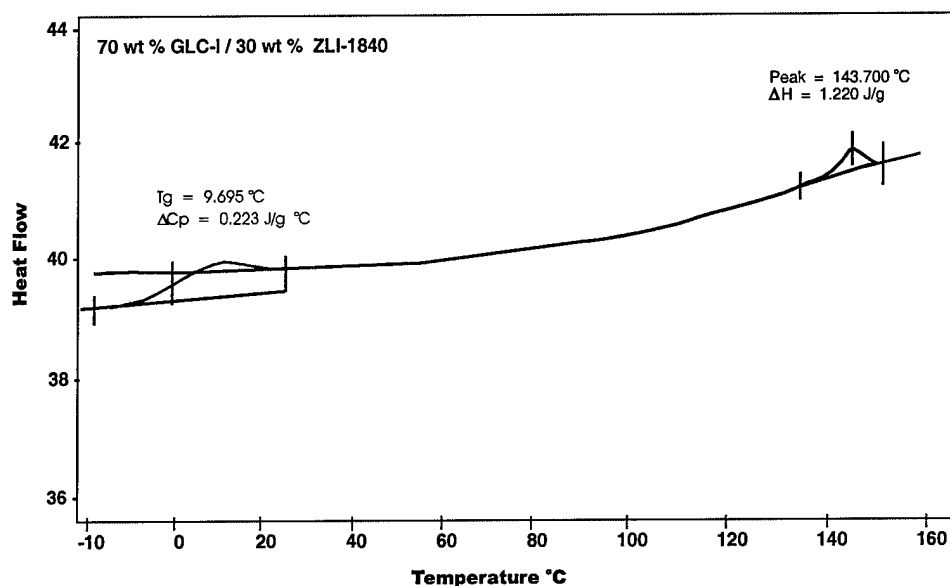


Figure 6: DSC measurement of 70 wt% GLC-I and 30 wt% ZLI-1840

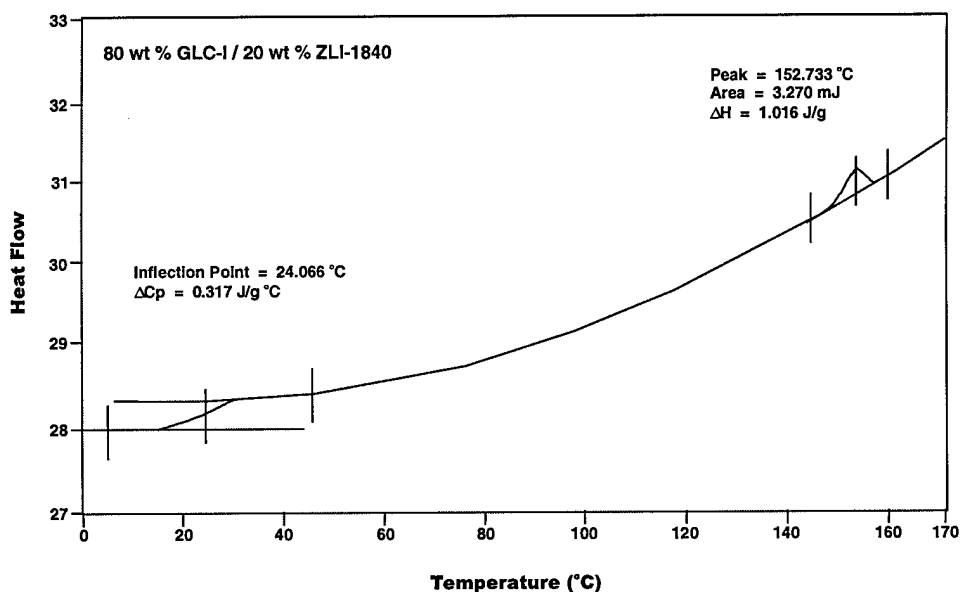


Figure 7: DSC measurement of 80 wt% GLC-I and 20 wt% ZLI-1840

### 3.2 Materials Processing

One important aspect in utilizing GLC materials for photonic devices is the need for the GLC materials to align with a surface alignment layer. Typically, GLC materials are aligned using a shear processing technique where one substrate is shifted back and forth with respect to the other substrate with the GLC material sandwiched between the substrates at a temperature above  $T_g$ . Shearing the GLC material aligns the LC molecules with the surface along the shear direction. In a bi-stable photonic device, shearing will not be available when the device is switched back and forth between its two states. It is therefore necessary to use another molecular alignment technique.

In conventional LC device design an alignment layer is used to force the LC molecules at the interface to align in a uniform direction. One common approach to surface alignment is to use a buffed polymer layers. We proposed to utilize a similar approach to align GLC materials.

During Phase-I, a several parallel-aligned cells were fabricated using GLC-IV, GLC-I and mixtures of GLC-I with ZLI-1840. The gap spacings varied between 4 and 14-microns. In the parallel-aligned cell the buff direction of each window surface is the same. This drives all the GLC molecules to align in the same direction throughout the cell creating a birefringent plate. The degree and uniformity of alignment can be easily observed between crossed polarizers. The sample fabricated showed a high degree of alignment and the only defects observable could be traced back to surface scratches on the substrate.

GLC samples were also fabricated using a high-temperature vacuum filling technique. In these experiments, empty, commercially supplied "bottles" were filled with various GLC materials. The development of the vacuum filling process may be important in the development of low-cost GLC-based devices.

### **3.3 Optical Properties**

Several significant results were obtained during Phase I of this STTR contract. Figure 2 shows the transmission spectra for pure GLC-I. This demonstrates the necessary optical clarity throughout the visible and near infrared for the majority of fiber-optic device applications. Key wavelengths of interest for fiber-optic applications include 890, 1320 and 1500 nm.

A detailed experimental plan was developed and carried out to measure the wavelength dependent optical birefringence of GLC-I and GLC-IV as a function of temperature and applied voltage. Figure 8 shows the optical system designed for this experiment. A fiber couple halogen lamp is used as a high brightness, broadband spectral source. The broadband light is collimated through a polarizer, the sample, and an analyzer using a 10x achromatic microscope objective with a numerical aperture of 0.25. The polarizer and analyzer are Glan-Thompson devices, which have an extinction ratio of  $10^5$ . The sample is mounted in a custom sample holder that is heated using cartridge heaters and controlled using an Omega temperature control unit. This temperature controlled sample holder can be mounted with the fast axis in four different orientations: -45, 0, 45 and 90 degrees. Transmitted light is collected using a matched achromatic microscope objective. Both objectives are mounted on kinematic mounts to ensure efficient coupling between the fibers. The collected light is then transmitted into an Ocean Optics solid-state spectrometer unit. Two bands are available on the purchased unit. The first band covers the spectral region from 350-900 nm with a spectral resolution of about 1.5 nm. The second band cover the spectral region from 750-1050 nm with a spectral resolution of less than 0.5 nm. The first band will be used to measure the birefringence throughout the visible spectrum and the second band will be used to measure both the NIR properties of the material as well as the fringes of the empty cells to determine cell thickness. The Ocean Optic Spectrometer unit is controlled from a standard PC computer and provided software. The spectral information acquired on each sample can be easily transferred into a spreadsheet for further data analysis, graphing, and materials property extraction.



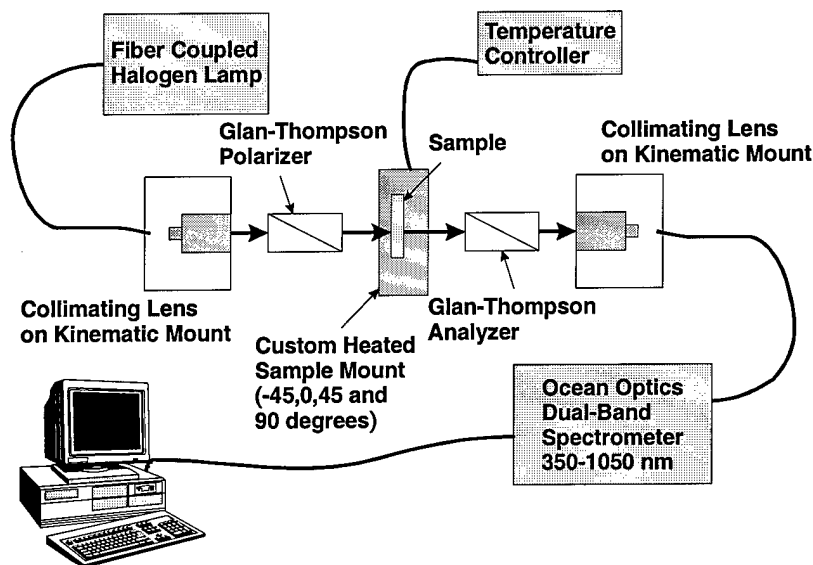


**Figure 8: Experimental configuration to measure  $d\Delta n(T,V,\lambda)$**

The collection of spectral information of a parallel-aligned GLC cell between a pair of high-performance polarizers enabled us to determine the optical birefringence as a function of wavelength by measuring the phase retardation through a GLC cell. The phase retardation ( $\delta$ ) is expressed as

$$\delta(V,T,\lambda) = 2\pi d\Delta n(V,T,\lambda)/\lambda,$$

where  $d$  is the GLC layer thickness;  $\Delta n(V,T,\lambda)$  is the effective LC birefringence, which is dependent on the applied voltage, temperature and wavelength ( $\lambda$ ) of the incident light. The normalized transmission of the cell situated between the polarizer and analyzer is given by

$$T_{//} = 1 - \sin^2(2\theta) \sin^2(\delta/2),$$

$$T_{\perp} = \sin^2(2\theta) \sin^2(\delta/2),$$

where  $//$  and  $\perp$  represent that the polarizer is parallel and perpendicular to the analyzer, respectively, and  $\theta$  is the angle between the axis of polarization and the fast-axis of the birefringent cell. When  $\theta = 45^\circ$ ,  $T_{//}$  and  $T_{\perp}$  are simplified to

$$T_{//} = \cos^2(\delta/2),$$

$$T_{\perp} = \sin^2(\delta/2).$$

Based on this theory we will be able to measure  $\Delta n(V,T,\lambda)$  by acquiring a series of spectra at different temperatures and voltages for GLC cells of a few different thicknesses. Although a unique solution exists for  $\Delta n(V,T,\lambda)$  from a single sample, it is important to use at least two thicknesses of cells to reduce measurement error and probe the impact of the surface alignment layer. Figure 9 shows the calculated transmission through a 10-micron thick cell and Figure 10 shows the calculated transmission through a 2-micron thick cell. Figure 11 shows the measured and calculated transmission through a 11.25-micron thick cell. The birefringence as a function of wavelength was calculated from this spectral data and the equations (4) and (7).

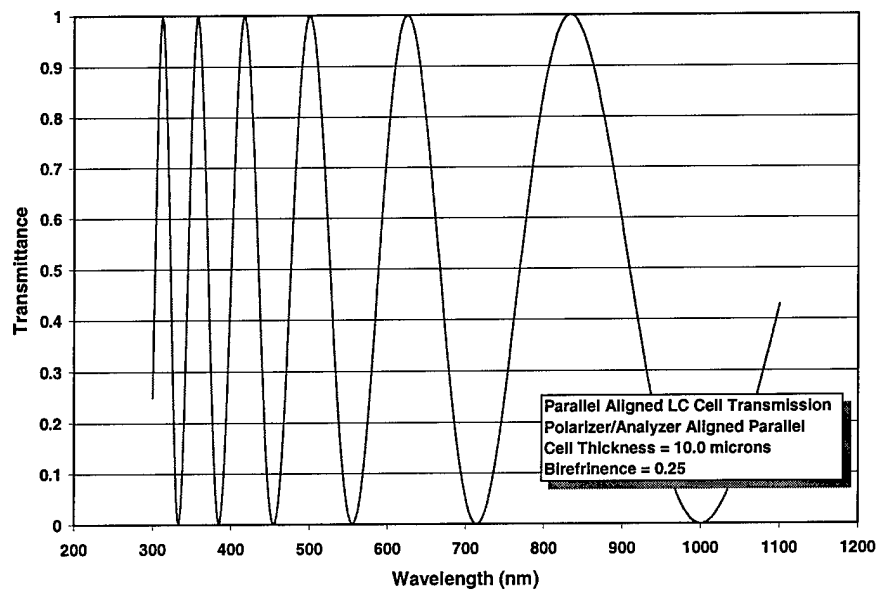


Figure 9: Predicted transmission through a 10-micron thick GLC parallel-aligned cell.

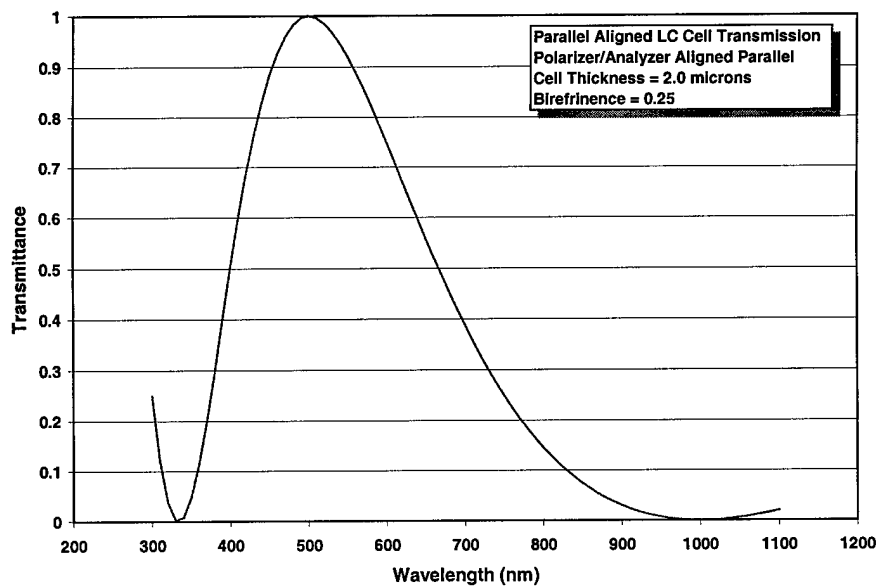
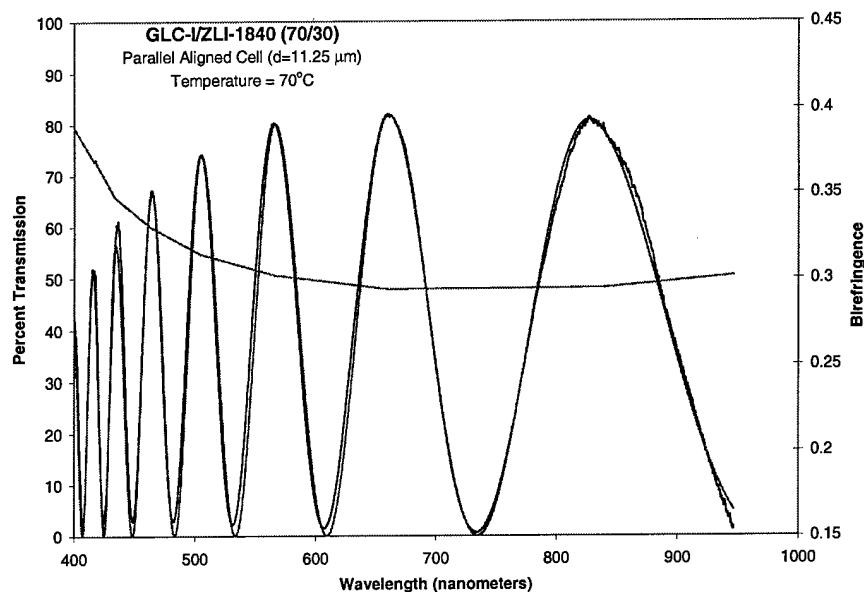
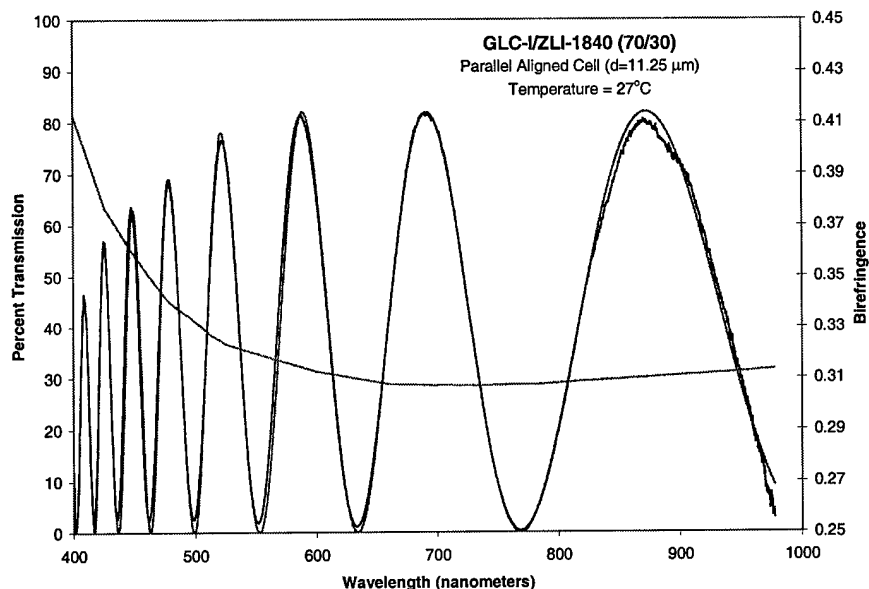


Figure 10: Predicted transmission through a 2-micron thick GLC parallel-aligned cell.



**Figure 11: Measured and calculated transmission spectra for 70% GLC-I and 30% LMM-LC at  $70^\circ\text{C}$ . The calculated data is based on the shown best-fit birefringence data.**

A series of data as was acquired on a parallel-aligned cell as a function of temperature. Figures 12a-12d show some of the results of these experiments. In these figures the calculated performance (red line) is fit to the measured data (blue line) by adjusting the optical birefringence (purple line). The calculations were made using the equation for  $T_{\parallel}$  shown above. Figure 13 shows a compilation of the birefringent data on this sample. As is characteristic with LC materials the birefringence increases rapidly as the wavelength decreases.



**Figure 12a: Measured and calculated transmission spectra for 70% GLC-I and 30% LMM-LC at  $27^\circ\text{C}$ . The calculated data is based on the shown best-fit birefringence data.**

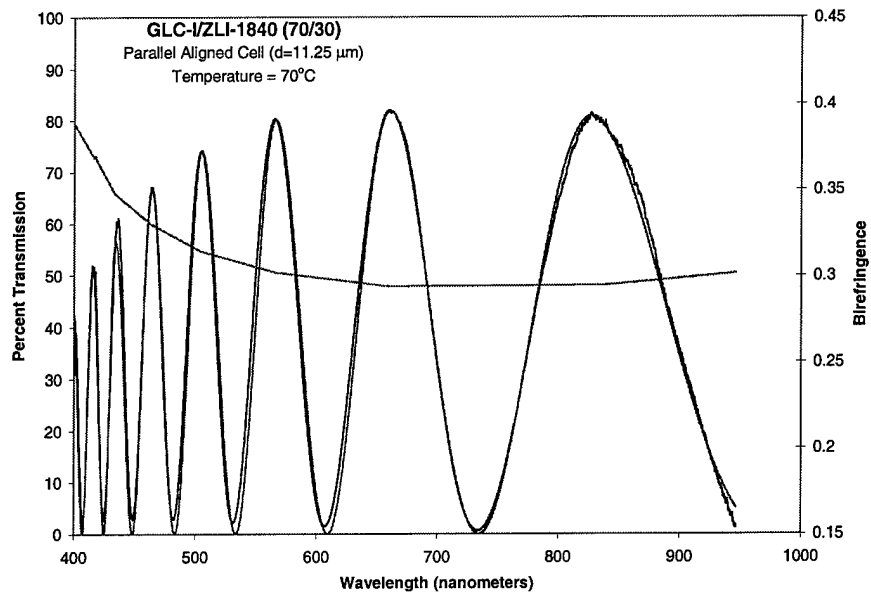


**Figure 12b: Measured and calculated transmission spectra for 70% GLC-I and 30% LMM-LC at  $70^\circ\text{C}$ . The calculated data is based on the shown best-fit birefringence data.**

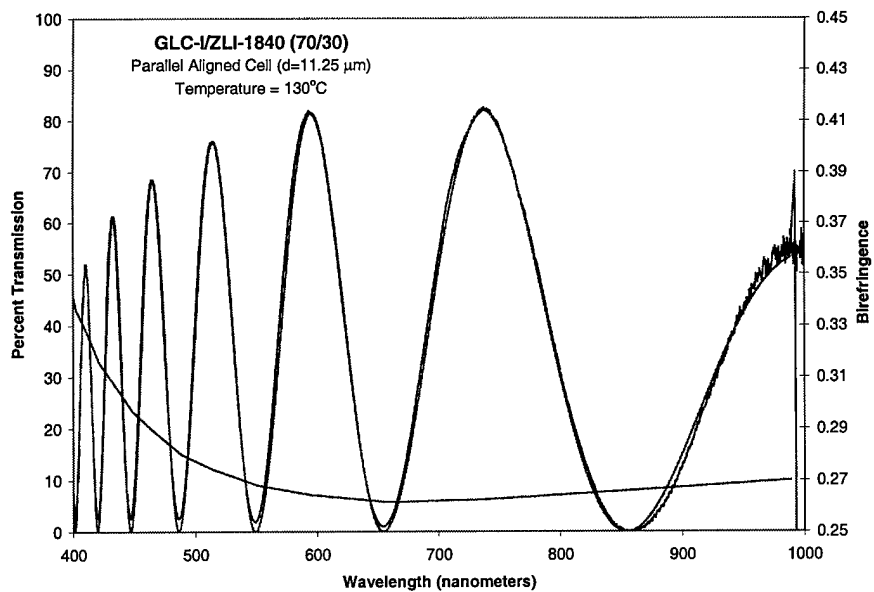


**Figure 12c: Measured and calculated transmission spectra for 70% GLC-I and 30% LMM-LC at  $130^\circ\text{C}$ . The calculated data is based on the shown best-fit birefringence data.**

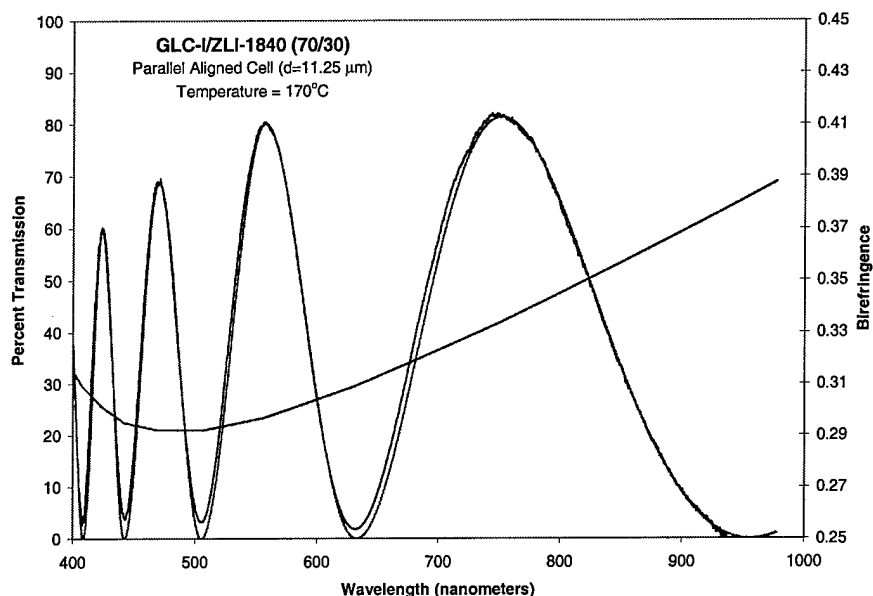


**Figure 12d: Measured and calculated transmission spectra for 70% GLC-I and 30% LMM-LC at 170°C. The calculated data is based on the shown best-fit birefringence data.**

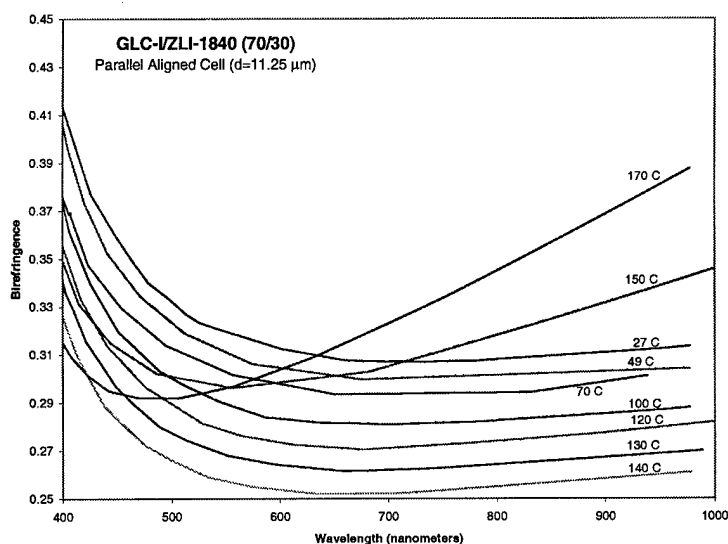


**Figure 13: Optical birefringence of 70% GLC-I and 30% LMM-LC as a function of wavelength from 27-170°C.**

The birefringent data shows that as the temperature is increased the birefringence decreases up until the around 140°C, after which, the birefringence rapidly increases with considerable wavelength dispersion. Figure 14 and Figure 15 shows that the temperature dependent optical properties start to deviate from linearity at about 120°C. This large change in materials properties over a narrow temperature span indicates that there are some physical phenomena at the molecular level that we currently do not understand taking place. These phenomena may be a result of mixing a LMM-LC with a GLC material or an inherent characteristic of the GLC material. Temperature-dependent birefringence

measurements on pure GLC-I will be conducted during the last two months of the Phase I program to gain greater insight into the source of this strong temperature dependence below the clearing temperature.

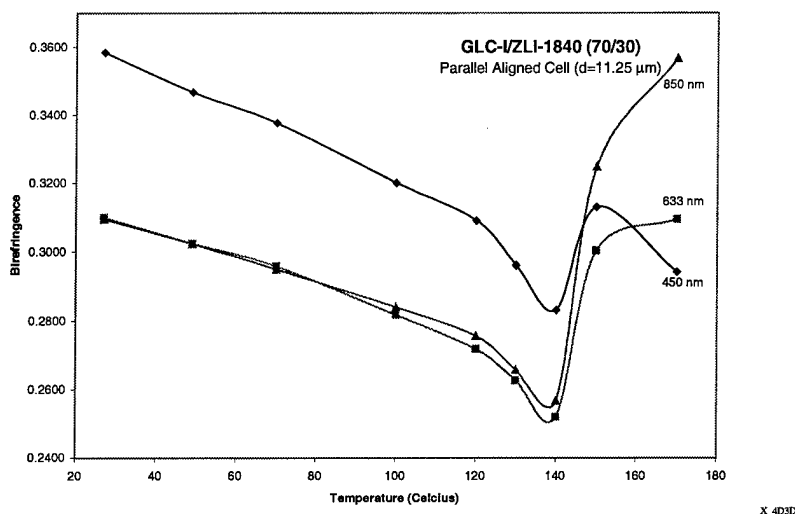


**Figure 14: Optical birefringence of 70% GLC-I and 30% LMM-LC as a function of temperature for three (3) discrete wavelengths (450nm, 633nm and 850nm).**

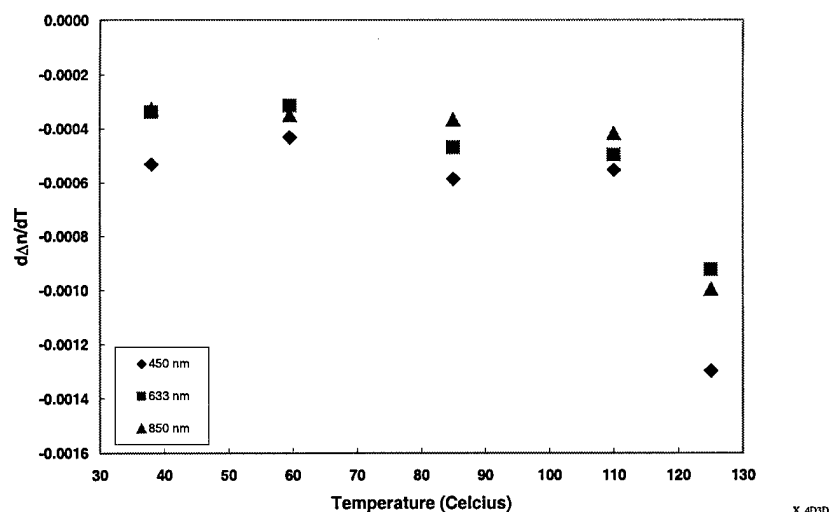


**Figure 15: Temperature dependence of optical birefringence ( $d\Delta n/dT$ ) at 450nm, 633nm and 850nm.**

In addition, preliminary experimental results of the optical properties of pure GLC-I showed no temperature dependent birefringence ( $d\Delta n/dT$ ) between room temperature and 60°C. Figure 16 shows the transmission spectra and calculated birefringence properties of a parallel aligned cell at 20°C and 60°C. This finding is significant in that many device designs use the birefringence properties of the material to achieve their functionality. *Therefore, the optical performance of devices based on this material will be temperature independent under normal operating conditions – a very important feature for many real-world applications.*

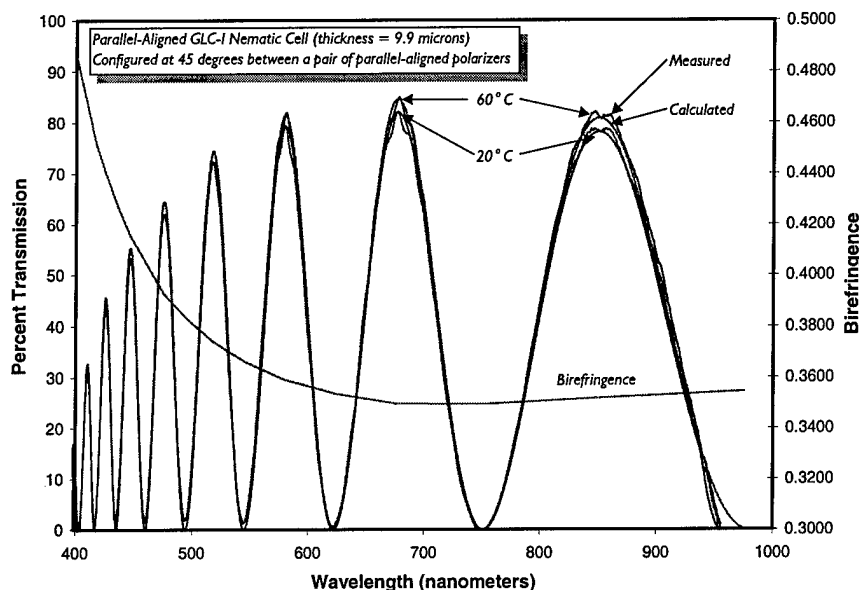


**Figure 16: Temperature Dependent Birefringence of pure GLC-I.**

### **3.4 Device Demonstration**

During the Phase I effort we investigated two different device configurations – a twisted nematic latching switch and a latching parallel-aligned device. A twisted nematic switch is capable of rotating the polarization throughout the spectra. This results in this device being suitable as a grey-level control. The parallel-aligned device is in essence a tunable waveplate with a spectral performance similar to that used to calculate the birefringence properties of the materials described above.

#### **3.4.1 Twisted Nematic (TN) Latching Switch**

The primary objective in the Phase I effort was to demonstrate an electrooptical latching optical switch device. This was demonstrated using mixtures of GLC and low molar mass liquid crystal (LMM-LC) materials. The device consisted of a twisted-nematic (TN) cell filled with a GLC/LMM-LC mixture consisting of 70 wt% GLCI and 30 wt% ZLI-1840. Mixtures were used early in the Phase I effort in order to facilitate sample preparation, however, mixing a LMM-LC with a GLC significantly reduced  $T_g$ .  $T_g$  for the 70-30 mixture was measured at 10°C. The low  $T_g$  resulted in the device relaxing from the latched state over a period of a few days. Figure 17 shows the spectral transmission through the TN device in both the switched and unswitched state at room temperature and no voltage applied. In this experiment, a TN LC cell was positioned between two parallel-aligned polarizers. In the fully relaxed state, the TN cell rotates the polarization of the incident light by 90° so that the analyzer blocks it. The relaxed state can be set by heating the TN cell to a temperature above the melting point of the GLC and below the clearing temperature without the application of any voltage. The switched- (or open-) state is achieved by orienting the LC molecules perpendicular to the TN cell surfaces. Applying a voltage across the TN cell rotates the molecules into this orientation. This can only be accomplished at temperatures above  $T_g$ . Latching is accomplished by cooling the material to a temperature below  $T_g$  (into the solid state) and removing the voltage.

### 3.4.2 Latching Parallel-Aligned GLC Device

Several samples were fabricated using another mixture consisting of 80 wt% GLC-I and 20 wt% ZLI-1840. DSG measurements of the 80-20 mixture indicating  $T_g$  is 24°C. The increase in the GLC-I composition will increase  $T_g$  and thereby increase the long-term stability of the device in the switched (latched) state. The alignment layers were parallel aligned. The samples were filled using the elevated temperature vacuum-fill process developed under this program. These samples showed significantly greater stability at room temperature than previously measured samples fabricated using the 70/30 mixture. Figure 18 shows the optical spectra of these samples in both the latched and relaxed state. The latched spectra shown here has been stable for over 2 weeks at room temperature.

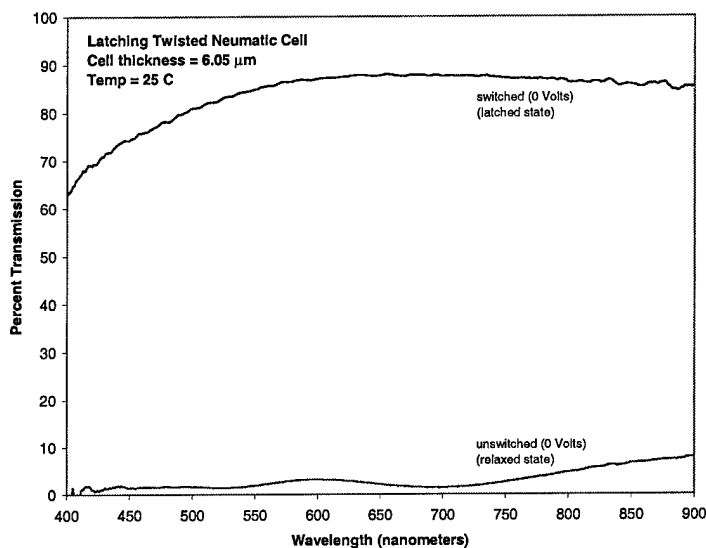


**Figure 17: Spectral transmission of a twisted nematic latching switch device. There is no voltage applied to the device in either the switched or unswitched state. This is the first-ever demonstration of a latching switch based on GLC materials technology.**

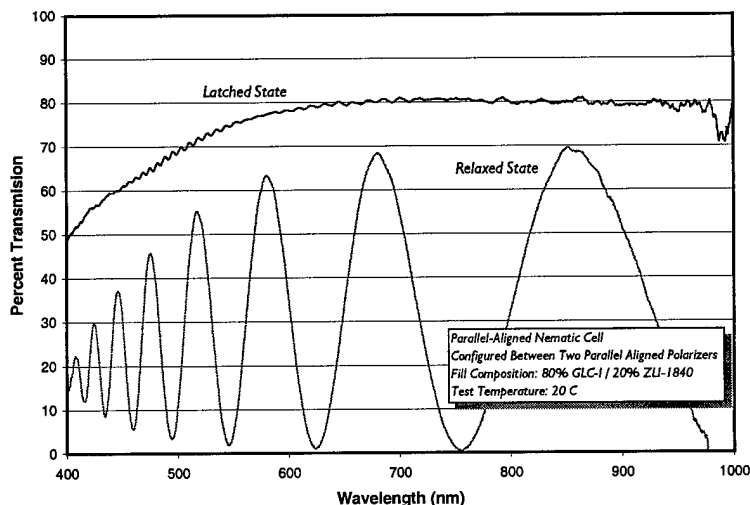


**Figure 18: Optical spectra of a parallel-aligned GLC-1/ZLI-1840 mixture (80%/20%) in both the latched and relaxed state with no voltage applied. These spectra demonstrate the stable electrooptical latching characteristics of this materials system.**



### 3.5 Technology Application

In the development of a new material system, it is important to maintain continuity between the materials research and the ultimate device applications. Therefore, in this program we propose to investigate the development of a commercially viable device using the GLC materials developed. Fiber optics is one application area where latching electrooptic device technology can make a significant impact. We have selected a latching, fiber-optic, variable attenuator as the device to be investigated under this program. This device was selected because the system requirements for such a device do not require high speeds or very demanding optical performance. In some applications, reconfiguration speeds on the order of 30 seconds are acceptable if the device is truly latchable. We believe that GLC technology will meet these requirements by the end of this Phase II program and position CRG for a Phase III commercialization of this product.

The device configuration selected for demonstrating the latching fiber-optic, variable attenuator is presented in Figure 20. In this polarization insensitive device, the incident beam is split into its principal polarizations using a birefringent beam displacer. These two beams are then passed through the GLC device that can modify the polarization state as needed to vary the transmitted power. The output beam is then recombined with a matched birefringent beam displacer. Such a device has been demonstrated using conventional low-molar-mass liquid crystals with acceptable performance for current system requirements.<sup>1</sup>

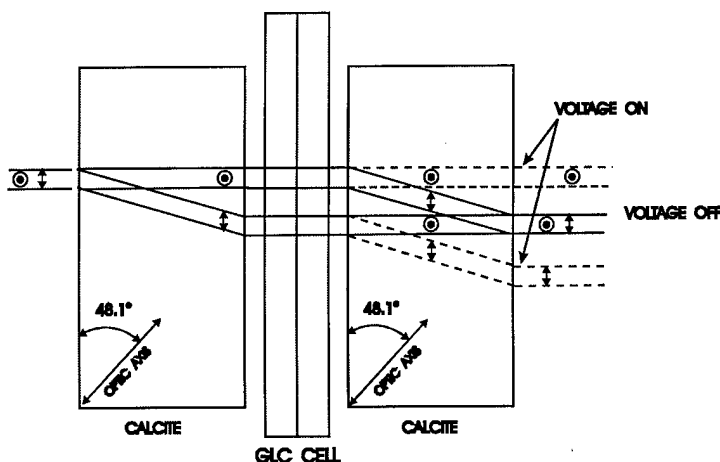


Figure 20: Latching variable fiber-optic attenuator design.

### 3.6 Materials Design

Our general concept of integrating two structurally dissimilar elements into a GLC system has been fruitful in creating a new class of organic materials. To elevate  $T_g$  beyond 100 °C that has been accomplished to date, we propose to adopt a more rigid core and a shorter spacer length. A case in point is Compound (II) compared to Compound (I) {GLC-IV} as depicted in Fig.1, indicating that a greater number of nematic pendants and/or a more rigid core, bicyclooctene vs cyclohexane, contribute to a higher  $T_g$  and a broader nematic temperature range,  $T_c - T_g$ . We have also demonstrated that both adamantane and cubane cores are capable of producing nematic, smectic, and cholesteric GLCs<sup>2,3</sup>, and both cores will be included as part of our effort to elevate  $T_g$ . Two additional approaches to elevating  $T_g$  will be implemented: (i) through intermolecular hydrogen bonding made possible by replacing the ester linkage between a pendant and its core with an amide linkage, and (ii) by using a hybrid core which will admit more pendants per molecule and will increase the molecular volume over a single core. The proposed strategies are as summarized in Figure 19 in terms of structural elements.

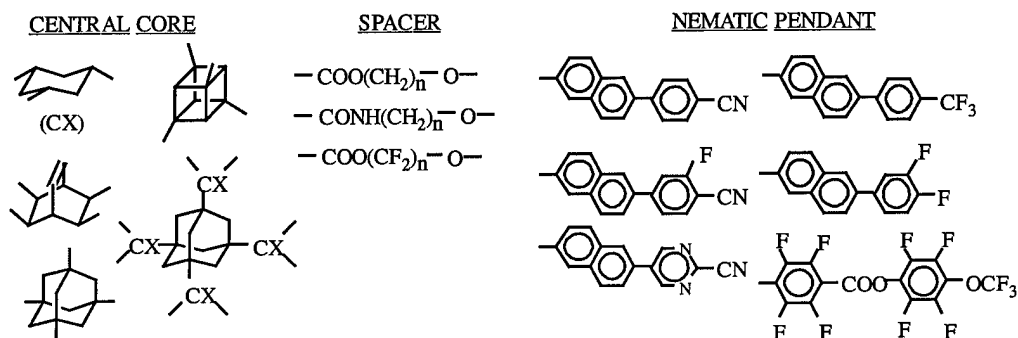


Figure 19: Nematic GLCs proposed for Phase II program.

## 4 Conclusions

Based on the experimental results presented in this report we believe this program successfully demonstrated that GLC materials have potential as a latching electrooptic material. Experiments have clearly demonstrated that GLC-I is suitable for some latching applications. Experiments have also identified several materials properties that must be improved before these materials can be implemented in photonic devices. These properties include an increased order parameter to increase the optical density between crossed polarizers and switching speed at temperatures above  $T_g$ . A phase II program would focus on integrating fluorinated nematic pendants into the GLC materials that have been developed for high-speed conventional LC applications. It may also be important to increase  $T_g$  to 80°C for some telecommunication and military applications.

## 5 References

- <sup>1</sup> E.G. Hanson, "Polarization-independent liquid-crystal optical attenuator for fiber-optics applications," *Appl. Opt.*, Vol. 21, No. 7, pp1342-1344 (1 April 1982).
- <sup>2</sup> S. H. Chen, J. C. Mastrangelo, H. Shi, A. Bashir-Hashemi, J. Li, and N. Gelber, "Novel Glass-Forming Organic Materials. 1. Adamantane with Pendant Cholesteryl, Disperse Red 1, and Nematogenic Groups," *Macromolecules* **28**, 7775 (1995).
- <sup>3</sup> S. H. Chen, J. C. Mastrangelo, T. N. Blanton, and A. Bashir-Hashemi, "Novel Glass-Forming Organic Materials. 3. Cubane with Pendant Nematogens, Carbazole, and Disperse Red 1," *Macromolecules* **30**, 93 (1997).